ACTA ABP BIOCHIMICA POLONICA

Vol. 70, No 3/2023
623–631
https://doi.org/10.18388/abp.2020_6721

Regular paper

An mRNA-based reverse-vaccinology strategy to stimulate the immune response against *Nipah virus* in humans using fusion glycoproteins

Muhammad Naveed[1]✉, Sarmad Mahmood[1], Tariq Aziz[2]✉, Muhammad Hammad Arif[1], Urooj Ali[1,3], Faisal Nouroz[4], Christos Zacharis[2], Metab Alharbi[5], Abdulrahman Alshammari[5] and Abdullah F. Alasmari[5]

[1]Department of Biotechnology, Faculty of Science and Technology, University of Central Punjab, Lahore, 54590 Pakistan; [2]Department of Agriculture, University of Ioaninna Arta, 47132 Greece; [3]Department of Biotechnology, Quaid-I-Azam University Islamabad, 45320 Pakistan; [4]Department of Bioinformatics, Hazara University Mansehra, 21300 Pakistan; [5]Department of Pharmacology and Toxicology, College of Pharmacy, King Saud University,11451 Riyadh, Saudi Arabia

The zoonotic pathogen, Nipah virus, is considered a potential healthcare threat due to its high mortality rates and detrimental symptoms like encephalitis. Ribavirin, an antiviral drug helps in overcoming the number of casualties and reducing the mortality rate, but no long-lasting solution has been proposed yet putting global health security in jeopardy. Given the cognizance of mRNA-based vaccines as safe and efficacious preventative strategies against pathogens, the current study has utilized the reverse-vaccinology approach coupled with immunoinformatics to propose an mRNA-based vaccine candidate against the Nipah virus. To ensure the effectiveness of the vaccine candidate against all strains of Nipah and associated viruses, three fusion glycoproteins from Nipah and Hendra viruses were selected. A total of 30 potential epitopes, 10 B-cell-, 10 MHC-I-, and 10 MHC-II-specific, were screened for the construct. The finalized epitopes were highly antigenic with scores ranging from 0.75 to 1.7615 at a threshold of 0.4 for viruses and non-homologous to *Homo sapiens* eradicating any chance of immune tolerance. The construct, with a World population coverage of 97.2%, was structurally stable, thermostable, and hydrophilic with indices of 32.91, 93.62, and –0.002, respectively. The vaccine candidate's tertiary structure was predicted with a TM score of 0.131 and the refined model displayed superlative RAMA improvement (98.2) and MolProbity score (0.975). A quality factor of 93.5421% further validated the structural quality and stability. A prompt and stable immune response was also simulated, and the vaccine candidate was shown to eliminate from the body within the first five days of injection. Immune complexes count of 7000 mg/mL was predicted against the antigen with a small but non-significant danger signal, countered by the cytokines. Lastly, strong molecular interactions of the vaccine candidate with TLR-3 (331.09 kcal/mol) and TLR-4 (-333.31 kcal/mol) and molecular dynamics simulation analysis authenticated the immunogenic potential of the vaccine candidate. This vaccine candidate can serve as a foundation for future *in-vitro* and *in-vivo* trials to minimize or eradicate the diseases associated with the Nipah virus or the Henipaviral family.

Keywords: nipah virus, hendra virus, fusion glycoproteins, immunoinformatics, reverse-vaccinology

Received: 06 March, 2023; revised: 17 April, 2023; accepted: 15 July, 2023; available on-line: 17 September, 2023

✉e-mail: dr.naveed@ucp.edu.pk (MN); iwockd@gmail.com (TA)

Acknowledgements of Financial Support: The authors greatly acknowledge and express their gratitude to the Researchers Supporting Project number (RSP2023R 462), King Saud University, Riyadh, Saudi Arabia.

Abbreviations: CDC, Centers for Disease Control; NHV, Nipah and Hendra viruses; SARS-Cov-2, Severe Acute Respiratory Syndrome Coronavirus 2

INTRODUCTION

Nipah Viral Disease is a zoonotic disease that has a high mortality rate of 91% (Pillai *et al*., 2020). The disease first emerged in 1998 in Malaysia and spread to neighboring countries including South-East Asia, like Bangladesh, Singapore, and India (Aditi & Shariff, 2019). It was isolated and identified at the University of Malaysia, Faculty of Medicine in 1999. As this virus was first spread in the Malaysian village Sungai Nipah, in pig farms and people associated with them, so scientists named this virus as Nipah virus (Pillai *et al*., 2020). This virus belongs to the Paramyxoviridae family and genus Henipa viruses. This virus is classified into two strains, the first one was isolated from Malaysia and Cambodia, and the other one was isolated from India and Bangladesh (Mourya *et al*., 2018). This virus leads to the development of rapid progressive illness in the human respiratory tract and causes encephalitis in the brain. Initially, because of the encephalitis-related symptoms, scientists thought of this disease as Japanese encephalitis, but it was confirmed later that the Nipah virus causes a different disease (Singh *et al*., 2019). The main host reservoirs for Henipa viruses are fruit bat *Pteropus*. These bats manipulate different fruits like date palms by secreting saliva and urine that is further consumed by animals. The most recent outbreak ruptured in Kerala, India with a loss of 17 human lives (Weingartl *et al*., 2009). The Nipah virus causes severe breathing issues, destroying the human lung structures and the membrane of the cerebrum. In this condition, the brain enlarges, causing memory loss and severe pain (Rockx *et al*., 2010). Its symptoms include brain encephalitis, headache, muscular pain, and respiratory disorders. Nausea, giddiness, and fever are also clinically significant (Reddy, 2018). According to the Centers for Disease Control (CDC), the Nipah virus has the potential to create a global emergency and, hence, deserves the immediate attention of the scientific community (Fischer *et al*., 2018). Ribavirin, an antiviral drug helps in overcoming the number of casualties and reducing the mortality rate,

but no long-lasting solution has been proposed yet (Deb *et al*., 2019). Vaccines are an efficacious solution to fight this deadly viral agent. mRNA-based vaccines are among the most effective candidates utilized to develop protective immunity against the pathogen. The vaccine shots activate the immune system, and the B-cells and T-cells develop immunologic memory for when a real pathogen attacks the host the immune system recognizes and destroys it. The mRNA vaccines are further appreciated for being cost-effective and timesaving (Kumar *et al*., 2015). With computational approaches, the labor intensity and process complexity are minimized (Naveed *et al*., 2022; Naveed *et al*., 2023a; Naveed *et al*., 2023b), making mRNA vaccines worthy solutions against viruses like the Nipah virus.

The current work is based on the proposition of an mRNA vaccine utilizing *in-silico* and immunoinformatics tools. The computational approach is considered to safely predict the immune response against the proposed vaccines. Three transmembrane proteins of the Nipah virus were selected for their significant role in the early interactions with the hosts. The selection of the transmembrane proteins was based on their antigenicity, allergenicity, non-toxicity, and non-resemblance with human proteins. Potential epitopes following the criteria of Naveed and others (Naveed *et al*., 2022a; Naveed *et al*., 2022b) are shortlisted and the construct is evaluated based on its population coverage, immune response simulations, molecular docking with respective toll-like receptor(s), and physicochemical properties.

MATERIALS AND METHODS

Selection of Target Proteins

The Nipah and Hendra Henipavirus genomes were retrieved from the NCBI database and downloaded in FastA format. CELLO2GO, an online server available at (http://cello.life.nctu.edu.tw/cello2go/), was utilized to study the gene ontology and localization of all the proteins present in the genomes. The conservation and homology evaluation was performed using blastp available at (https://blast.ncbi.nlm.nih.gov/Blast.cgi?PAGE=Proteins). It ensured that the selected proteins based on protein localization are non-homologous to the human host and are conserved across Henipaviruses. Lastly, the online servers Vaxijen2.0, available at (http://www.ddg-pharmfac.net/vaxijen/VaxiJen/VaxiJen.html), and AllerTop, 2.0 accessed at (https://www.ddg-pharmfac.net/AllerTOP/method.html), were utilized to predict the antigenicity and allergenicity of the shortlisted proteins, respectively.

Protein Selection & Sequence Retrieval

The online server UniProt (www.uniprot.org) was used to retrieve the Nipah virus virulent protein sequences. Based on different factors like higher antigenic capacity, non-allergenicity, non-toxicity, and non-resemblance with *Homo sapiens*, three trans-membrane fusion glycoproteins (one belonging to Hendra virus and two belonging to the identified strains of Nipah virus) were selected for a potential vaccine candidate.

Prediction of B-cell Epitopes

ABCpred webserver (https://webs.iiitd.edu.in/raghava/abcpred/ABC_submission.html) was used for the prediction of B cell epitopes from each protein. We only selected the epitopes having non-allergenic, highly antigenic, and non-toxic analyses. We used the online server (https://www.ddg-pharmfac.net/AllerTOP/), Vaxijen 2.0 (http://www.ddg-pharmfac.net/vaxijen), and ToxinPred (http://crdd.osdd.net/raghava/toxinpred/), respectively. Moreover, we screened the predicted epitopes to see if they have homologs among humans and excluded the epitopes which might induce autoimmunity.

Prediction of the MHC-1 Epitopes

MHC-1 binding prediction tool of IEDB (http://tools.iedb.org/mhci/) was used to predict the conserved epitopes with the NetMHCpan BA 4.0 version (Reynisson *et al*., 2020). MHC source specie was selected as human and epitopes were screened based on higher antigenicity value, non-allergenicity, and a specified range of IC_{50} values lower than 100.

Prediction of MHC-II Epitopes

MHC-II binding prediction tool (http://tools.iedb.org/mhcii/) was used to predict the conserved epitopes. NetMHCIIpan 4.0 BA version (Reynisson *et al*., 2020) was utilized to predict the conserved epitopes. Epitopes were screened based on higher antigenicity value, non-allergenicity, and a specified range of IC_{50} values lower than 100.

Population Coverage

The evaluation of population coverage of the selected MHC-I and MHC-II epitopes was carried out with the IEDB population coverage tool (http://tools.iedb.org/population/). All the selected epitopes with their corresponding alleles were included in the input file. On the input page, the number of epitopes was changed accordingly. A combined MHC-I and MHC-II epitopes input file was provided, and the World was selected as the target population.

Vaccine Construct

The finalized epitopes of B- and T-cells were reverse-translated and fused together with the help of linkers, adjuvants, a MITD sequence, polyA-tail, 5' and 3' UTRs, and methyl-guanosine cap at the start of the construct to enable it for in-host expression.

Analysis of Physiochemical Properties

The physicochemical properties of the vaccine construct were predicted by the ProtParam tool of the ExPasy web server (https://web.expasy.org/protparam/). Toxicity prediction was done using Toxinpred. The Vaxijen tool was run to predict the antigenicity of the vaccine construct and to check the vaccine construct's allergenicity.

Prediction of Secondary Structure of the Proposed mRNA Vaccine

PSIPRED (http://bioinf.cs.ucl.ac.uk/psipred/) was used for the prediction of the secondary structure. The mRNA vaccine candidate sequence was first translated to its primary protein sequence using EXPASY translate, and this primary sequence was used as an input sequence on PSIPRED. Out of a variety of analyses available on the server, the cartoon structure along with the basic prediction was interpreted.

Prediction and Refinement of the Tertiary Structure

The tertiary structure of the mRNA was predicted using the online server trRosetta https://yanglab.nankai.edu.cn/trRosetta/. This online server for protein docking has been continuously extended and refactored. Its advantages include interoperability between modeling capabilities and performance (Leman *et al.*, 2020). Refinement of the tertiary structure of our proposed mRNA vaccine was done by Galaxy WEB's Galaxy REFINE https://galaxy.seoklab.org/.

Validation of Tertiary Structure of the Proposed mRNA Vaccine

After refinement of the tertiary structure, we validated our proposed mRNA tertiary structure by Ramachandran plot analysis using the PROCHECK server (https://saves.mbi.ucla.edu/), whereas the structure quality was validated using ERRAT quality score on the PROCHECK server.

Immune Simulations

To validate whether the mRNA-based vaccine construct has the potential to elicit a stable immune response, C-IMMSIM analyses were performed through the webserver available at https://kraken.iac.rm.cnr.it/C-IMMSIM/index.php?page=1. An immunogenic response of single-dose injection was calculated.

Molecular Docking and Simulation Analysis

Molecular docking predicted the immune response stimulation capacity and molecular interaction between the proposed mRNA vaccine protein and toll-like receptors. HDOCK webserver (https://www.nature.com/articles/s41596-020-0312-x) was used. For this purpose, TLR-3 (PDB ID: 3ULV) and TLR-4 (PDB ID:4R7N) were retrieved from RCSB PDB (https://www.rcsb.org/). For simulation analysis of the docked complexes, iMODS (https://imods.iqfr.csic.es/) was utilized.

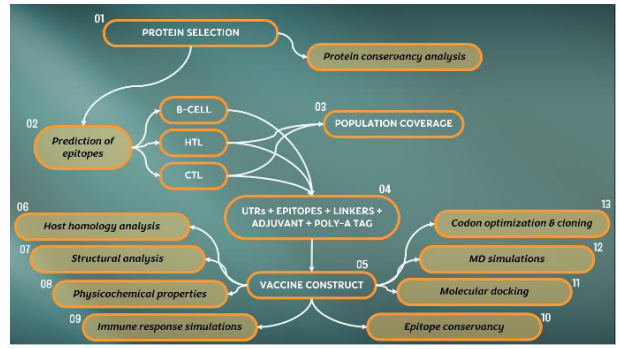

Figure 1. Process overview of the mRNA-based vaccine construct

Cloning of the Construct

The mRNA-based construct was converted into the DNA sequence after codon optimization using JCAT (http://www.jcat.de/Result.jsp). The optimized construct was cloned in the pBluescribe vector at the BsoB1 site with the removal of overhangs using Snapgene https://www.snapgene.com/. The methodology is schematically represented in Fig. 1.

RESULTS

Target Proteins' Selection

Analyzing 2335 proteins present in the genomes of Nipah and Hendra Henipavirus on the CELLO2GO tool, we selected several pathogenic transmembrane proteins. Out of 108 transmembrane proteins, 3 transmembrane proteins were selected for vaccine design.

Selection and Sequence Retrieval of Transmembrane Proteins

Based on different factors like higher antigenic capacity, non-allergenicity, non-toxicity and non-resemblance with a human protein, three transmembrane fusion glycoproteins

Table 1. List of selected transmembrane proteins for vaccine design against the Nipah virus

Accession ID	Protein name	Antigenicity	Allergenicity	Toxicity
Q9IH63 (Nipah virus)	Fusion glycoprotein F0	0.5012	Non-Allergen	Non-toxic
O89342 (Hendra virus)	Fusion glycoprotein F0	0.5534	Non-Allergen	Non-toxic
A0A1L7B8D7 (Nipah)	Fusion glycoprotein F0	0.5056	Non-Allergen	Non-toxic

Table 2. List of Predicted B-cell Epitopes for vaccine design

Protein	Epitope	Antigenicity	Allergenicity
1	LGSVNYNSEGIAIGPP	1.1587	Non-Allergen
	GVAIGIATAAQITAGV	0.9828	Non-Allergen
	SRLEDRRVRPTSSGDL	1.0553	Non-Allergen
2	YVQELLPVSFNNDNSE	0.6083	Non-Allergen
	GITRKYKIKSNPLTKD	0.6437	Non-Allergen
	VGDVKLAGVVMAGIAI	0.8857	Non-Allergen
	KRGNYSRLDDRQVRPV	1.2056	Non-Allergen
	EGIAIGPPVFTDKVDI	0.7407	Non-Allergen
3	LSMIILYVLSIASLCI	0.8365	Non-Allergen
	KKRNTYSRLEDRRVRP	0.7484	Non-Allergen

Table 3. List of predicted MHC-I-restricted epitopes for vaccine design

Protein	Epitope	Antigenicity	Alleles
1	SLCIGLITFI	1.0498	HLA-A*02:03, HLA-A*02:01, HLA-A*02:06, HLA-A*68:02
	FISFIIVEKK	1.7539	HLA-A*68:01, HLA-A*11:01, HLA-A*03:01,
	TELSLDLAL	1.1768	HLA-B*40:01, HLA-B*44:03, HLA-B*44:02,
2	FISFVIVEK	1.4849	HLA-A*68:01, HLA-A*11:01, HLA-A*03:01,
	KSRLTGILS	0.7552	HLA-A*30:01, HLA-A*30:02
	IGLITFISFV	1.1281	HLA-A*02:03, HLA-A*02:01, HLA-A*02:06, HLA-A*68:02,
	RLKCLLCGI	1.5082	HLA-A*02:03, HLA-A*30:01, HLA-A*02:06, HLA-A*02:01, HLA-A*32:01, HLA-B*15:01
	FISFIIVEK	1.1861	HLA-A*68:01, HLA-A*11:01, HLA-A*03:01, HLA-A*33:01, HLA-A*31:01
3	KIKSNPLTK	0.725	HLA-A*30:01, HLA-A*03:01, HLA-A*11:01, HLA-A*31:01,
	SLCIGLITFI	1.0498	HLA-A*02:03, HLA-A*02:01, HLA-A*02:06, HLA-A*68:02, HLA-A*32:01, HLA-B*15:01

were selected for vaccine design. UniProt protein database was used for the sequence retrieval of fusion glycoproteins under specific allocated UniProt IDs given in Table 1.

Prediction of B cells Epitopes

After protein selection and their sequence retrieval, we screened the predicted B-epitopes according to their higher antigenic capacity, non-allergenicity, non-homology, and non-toxicity. Ten B-cells epitopes, shown in Table 2, extracted from three selected fusion glycoproteins were included in the vaccine construct. All the shortlisted epitopes were non-allergenic and antigenic with a score between 0.7 and 1.21, having a threshold of 0.4.

Prediction of MHC-1 Epitopes

For the prediction of MHC-I-restricted epitopes, all alleles of the HLA dataset were selected, and the peptide length was taken as 9 and 10. The epitopes were sorted based on predicted IC50 values. All other parameters were kept as default. The shortlisted epitopes were screened based on higher antigenicity value, allergenicity and an IC50 value <100 giving a total of 10 epitopes, provided in Table 3.

Prediction of MHC-II epitopes

The length of the predicted MCH-2 cell epitopes was set at 15 and all other parameters were kept as default. The predicted epitopes were saved as an XHTML output table and peptides are sorted according to their adjusted rank. Further screening relied upon antigenicity values and non-allergenicity. The finalized epitopes, shown in Table 4, having a higher antigenicity value, non-allergenicity and IC50 values <100 were selected for the vaccine construct. The restricting alleles for both the MHC-I-restricted and MHC-II-restricted epitopes were recorded for population coverage analysis.

Vaccine Construct

The screened epitopes with a cumulative World population coverage of 97.2%, shown in Fig. 6A, were converted to the mRNA sequence, and fused together using universal linkers (EAAAK, GPGPG, KK, AAY). The 5'

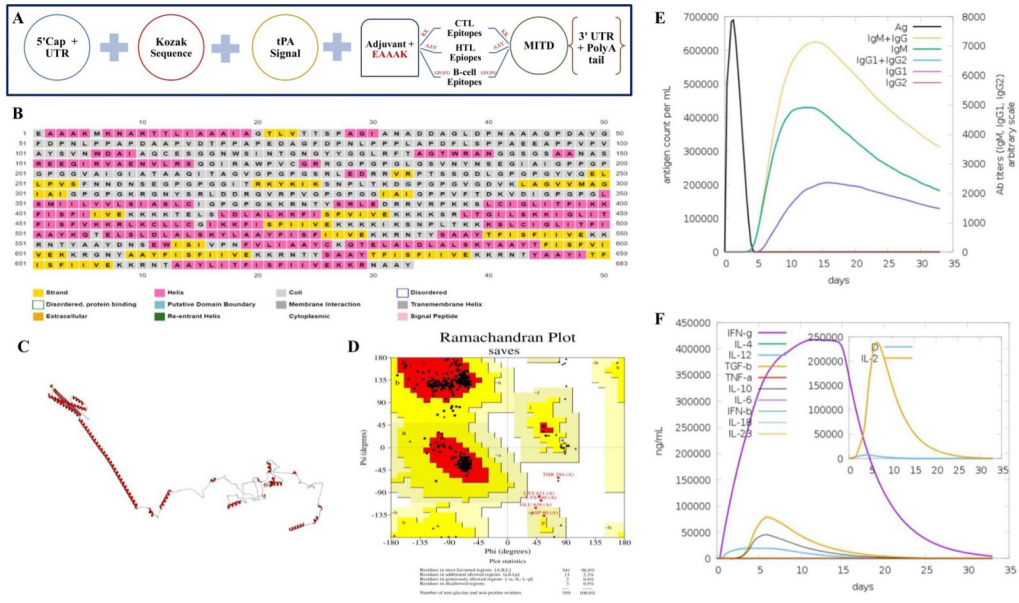

Figure 2. (A) The final vaccine construct; (B) The predicted secondary structure of the construct; (C) The predicted tertiary structure refined by GalaxyREFINE; (D) Ramachandran plot validating the refined tertiary structure; (E) Antigen and Immune complex counts plotted over a month period; (F) Danger signal produced by the body in response to the injection and the cytokines production plotted over a month.

Table 4. List of predicted MHC-II cell epitopes for vaccine design

Protein	Epitope	Antigenicity	Alleles
1	KQTELSL-DLALSKYL	0.8424	HLA-DRB1*03:01, HLA-DRB3*01:01, HLA-DRB1*07:01, HLA-DRB1*04:01, HLA-DRB5*01:01, HLA-DRB4*01:01, HLA-DRB1*13:02, HLA-DPA1*03:01/DPB1*04:02, HLA-DRB1*09:01, HLA--DRB1*15:01, HLA-DRB1*01:01, HLA-DRB1*04:05
	FISFIIVEK-KRNTYS	1.4463	HLA-DRB1*11:01, HLA-DRB1*08:02, HLA-DPA1*02:01/DPB1*05:01, HLA-DRB5*01:01, HLA--DRB4*01:01, HLA-DRB1*03:01, HLA-DPA1*03:01/DPB1*04:02, HLA-DRB1*12:01, HLA--DPA1*02:01/DPB1*01:01, HLA-DRB1*15:01, HLA-DRB1*13:02, HLA-DRB1*04:05, HLA--DRB1*04:01, HLA-DRB1*07:01, HLA-DRB1*01:01
	TFISFIIVEK-KRNTY	1.4822	HLA-DRB1*11:01, HLA-DPA1*02:01/DPB1*05:01, HLA-DRB1*08:02, HLA-DRB5*01:01, HLA--DRB4*01:01, HLA-DPA1*03:01/DPB1*04:02, HLA-DPA1*02:01/DPB1*01:01, HLA-DRB1*03:01, HLA-DPA1*01:03/DPB1*02:01, HLA-DRB1*12:01, HLA-DPA1*01:03/DPB1*04:01, HLA--DRB1*04:05, HLA-DRB1*15:01, HLA-DRB1*04:01, HLA-DRB1*13:02, HLA-DRB1*07:01, HLA--DRB1*01:01, HLA-DRB1*09:01
2	DNSEWISI-VPNFVLI	0.789	HLA-DRB1*15:01, HLA-DRB1*07:01, HLA-DRB1*12:01, HLA-DRB1*04:05, HLA-DRB1*13:02, HLA-DRB1*01:01, HLA-DRB1*09:01, HLA-DQA1*05:01/DQB1*02:01, HLA-DRB1*04:01, HLA--DPA1*01:03/DPB1*04:01, HLA-DPA1*03:01/DPB1*04:02, HLA-DPA1*02:01/DPB1*01:01, HLA--DPA1*01:03/DPB1*02:01, HLA-DRB1*08:02, HLA-DRB4*01:01
	CKQTELAL-DLALSKY	0.8828	HLA-DRB1*03:01, HLA-DRB3*01:01, HLA-DRB1*04:01, HLA-DPA1*03:01/DPB1*04:02, HLA--DPA1*02:01/DPB1*01:01, HLA-DRB5*01:01, HLA-DRB4*01:01, HLA-DRB1*13:02
	TFISFVIVEK-KRGNY	1.7615	HLA-DRB1*11:01, HLA-DRB1*08:02, HLA-DPA1*02:01/DPB1*05:01, HLA-DRB5*01:01, HLA--DPA1*03:01/DPB1*04:02, HLA-DPA1*02:01/DPB1*01:01, HLA-DRB4*01:01, HLA-DPA1*01:03/DPB1*02:01, HLA-DRB1*04:05, HLA-DRB1*04:01, HLA-DRB1*15:01, HLA-DRB1*07:01
3	FISFIIVEK-KRNTYS	1.4463	HLA-DRB1*11:01, HLA-DRB1*08:02, HLA-DPA1*02:01/DPB1*05:01, HLA-DRB5*01:01, HLA--DRB4*01:01, HLA-DRB1*03:01, HLA-DPA1*03:01/DPB1*04:02, HLA-DRB1*12:01, HLA--DPA1*02:01/DPB1*01:01, HLA-DRB1*15:01, HLA-DRB1*13:02, HLA-DRB1*04:05, HLA--DRB1*04:01, HLA-DRB1*07:01, HLA-DRB1*01:01
	TFISFIIVEK-KRNTY	1.4822	HLA-DRB1*11:01, HLA-DPA1*02:01/DPB1*05:01, HLA-DRB1*08:02, HLA-DRB5*01:01, HLA--DRB4*01:01, HLA-DPA1*03:01/DPB1*04:02, HLA-DPA1*02:01/DPB1*01:01, HLA-DRB1*03:01, HLA-DPA1*01:03/DPB1*02:01, HLA-DRB1*12:01, HLA-DPA1*01:03/DPB1*04:01, HLA--DRB1*04:05, HLA-DRB1*15:01, HLA-DRB1*04:01, HLA-DRB1*13:02, HLA-DRB1*07:01, HLA--DRB1*01:01, HLA-DRB1*09:01
	ITFISFIIVEK-KRNT	1.7597	HLA-DPA1*02:01/DPB1*05:01, HLA-DRB1*11:01, HLA-DRB5*01:01, HLA-DRB1*08:02, HLA--DPA1*03:01/DPB1*04:02, HLA-DPA1*02:01/DPB1*01:01, HLA-DRB4*01:01, HLA-DPA1*01:03/DPB1*04:01, HLA-DPA1*01:03/DPB1*02:01, HLA-DRB1*04:05, HLA-DRB1*12:01, HLA--DRB1*03:01, HLA-DRB1*15:01, HLA-DRB1*04:01, HLA-DRB1*07:01, HLA-DRB1*13:02, HLA--DRB1*01:01, HLA-DRB1*09:01,
	LITFISFIIVEK-KRN	1.5214	HLA-DPA1*02:01/DPB1*05:01, HLA-DRB1*11:01, HLA-DRB5*01:01, HLA-DRB1*08:02, HLA--DPA1*03:01/DPB1*04:02, HLA-DPA1*02:01/DPB1*01:01, HLA-DPA1*01:03/DPB1*04:01, HLA-DPA1*01:03/DPB1*02:01, HLA-DRB4*01:01, HLA-DRB1*04:05, HLA-DRB1*12:01, HLA--DRB1*15:01, HLA-DRB1*04:01, HLA-DRB1*07:01, HLA-DRB1*01:01, HLA-DRB1*13:02, HLA--DRB1*09:01

and 3' components along with the RpfE adjuvant and the Kozak sequence were added to the construct, shown in Fig. 1A, for stability, improved immunogenicity, and ease of entry into the host cells.

Physiochemical Properties Prediction

The physicochemical properties computed for the vaccine candidate by translating the construct into its peptide sequence indicated that it was antigenic (0.8746), non-allergenic, stable (32.91), thermostable (93.62), hydrophilic (-0.002), non-toxic, and had 683 amino acids. Table 5 discusses the analysis and indication of the physicochemical properties of peptides.

Prediction of Secondary Structure

The secondary structure predicted by PSIPRED, shown in Fig. 2B, depicts the alpha-helices, beta-turns, and coils of the vaccine candidate. Most of the amino acid residues were predicted as coils indicating the vaccine candidate's transmembrane localization.

Prediction and Refinement of Tertiary Structure

trRosetta predicted the tertiary model of the vaccine candidate with a TM-score of 0.131. Since, this was below the ideal TM score, the model was refined and GalaxyREFINE predicted 5 models, out of which the first one was selected (depicted in Fig. 2C) based on the most improved RAMA scores (98.2) indicating the torsion angle distribution of the vaccine candidate. Other metrics like MolProbity (0.975) that evaluates the model quality at both protein and nucleic-acid levels and least RMSD (0.356) calculating the difference in protein backbone conformation in the initial and final structures were also considered for model selection.

Validation of Tertiary Structure

ERRAT calculated the overall quality factor score of 93.5421 and the Ramachandran plot (Fig. 2D) indicated that most of the residues lie in the most favored region. 541 residues constituted 96.8% of the total protein, residues in the additional allowed region were 2.3%, in the generally allowed region were 0.4% and in the disallowed region were 0.5%.

Immune Simulation Response

C-IMMSIM predicted a potent and stable immune response against the injected antigen. The graph in Fig. 2E illustrates that the server predicted the antigen to be eliminated from the host system within the first 5 days

Table 5. The Physiochemical Properties of the proposed mRNA vaccine

Property	Measurement	Indication
Antigenicity	0.8746	Antigenic
Allergenicity	Non-Allergen	Non-Allergen
No. of Amino Acids	683	Appropriate
Formula	$C_{3337}H_{5316}N_{880}O_{933}S_{11}$	Appropriate
Total number of -ve charged residues (Asp + Glu)	52	–
Total number of +ve charged residues (Arg + Lys)	90	–
Theoretical pI	9.74	Basic
Estimated Half Life (mammalian reticulocytes)	1 hour	Easily eliminated
Instability Index	32.91	Stable
Aliphatic Index	93.62	Thermostable
Grand average of hydropathicity (GRAVY)	–0.002	Hydrophilic
Toxicity of Vaccine Construct	Non-toxic	Non-toxic

after escalating to 700 000 antigen count per mL on the first day. The immune complexes (IgG+IgM) were generated when the antigen count was almost 0 and escalated up to 7000 for the first 15 days of injection. The complex count decreased afterward but became steady at 3600 after a month indicating stability and longevity of the immune response. The graph in Fig. 2F illustrates the cytokine production and danger-signal produced by the body in response to the antigen. A small danger signal was produced lasting for up to 25 days but was not significant. The interleukin-2 count escalated up to 250 000 mg/mL on the 5th day and steadily decreased afterward. It was clear from the graph that the increase in IL-2 count was a direct response to the signal validating the potent response. IFN-gamma was also readily produced by the immune system.

Molecular Docking Analysis

HDOCK webserver predicted 10 models of the docking poses of mRNA vaccine construct with TLR-3 (PDB ID: 3ULV) and 10 models with TLR-4 (PDB ID:4R7N). With TLR-3 docking, the first model was selected having a docking score of –331.09 kcal/mol and a confidence score of 0.9740, shown in Fig. 3A. With TLR-4 docking, the first model (Fig. 3B) was selected for having a docking score of –333.31 kcal/mol and a confidence score of 0.975.

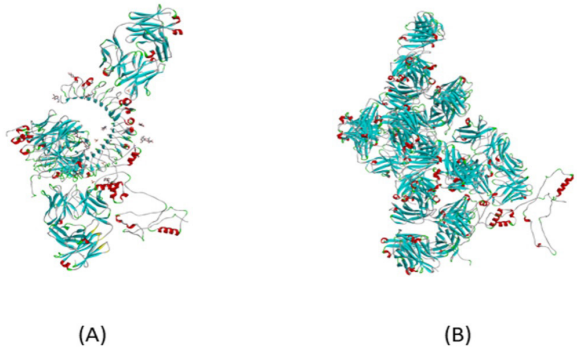

Figure 3. (A) Docking complex with TLR-3 (PDB ID: 3ULV); (B) docking complex with TLR-4 (PDB ID:4R7N)

Molecular Dynamics Simulations

With an eigenvalue of 2.95646e-06 and 4.0524e-06, illustrated in Figs. 4d and 5d respectively, the docked complex (Figs. 4a, 5a) was predicted to be stiff with little dynamic residues. The B-factor (shown in Figs. 4b and 5b) also showed minimal flexibility, except for the last few residues. The deformability plot shown in Figs. 4c and 5c was found consistent with the eigenvalue and the B-factor plot indicating that only a few residues towards the end of the docked complex were flexible/deformable. The variance and co-variance map (Figs. 4e, 5e and Figs. 4f and 5f, respectively) show stable amino acid-pair interactions validating strong molecular interactions. Lastly, the elastic network map showed that the atoms in the docked complex are closely linked to each other, demonstrated in Figs. 4g and 5g, reflecting on the covariance findings.

Expression Analysis

The CAI score of 0.95518 and GC content of 67.057% reflected the maximum codon optimization of the construct sequence, illustrated in Fig. 6B. pBluescribe plasmid was utilized for the *in-silico* cloning experiment. The plasmid was cut by the AHD-I enzyme producing sticky ends, enabling unidirectional cloning of the construct into the vector. Figure 6C shows the cloning process, whereas Fig. 6D represents the cloned vector.

DISCUSSION

Nipah virus first emerged in the late nineties, with fruit bat as its mediatory host. First, it was observed in the pig but was soon observed in the human population (Aditi & Shariff, 2019). Due to a high fatality rate in developing countries, this virus is thought to evoke a potential zoonotic pandemic like coronavirus (Kulkarni *et al.*, 2013). Ribavirin, a drug initially used against hepatitis and liver-virus infection, has been utilized to minimize viral load in Nipah viral disease patients (Deb *et al.*, 2019). However, the mortality rates are still high (Naveed *et al.*, 2021). Owing to the absence of preventative strate-

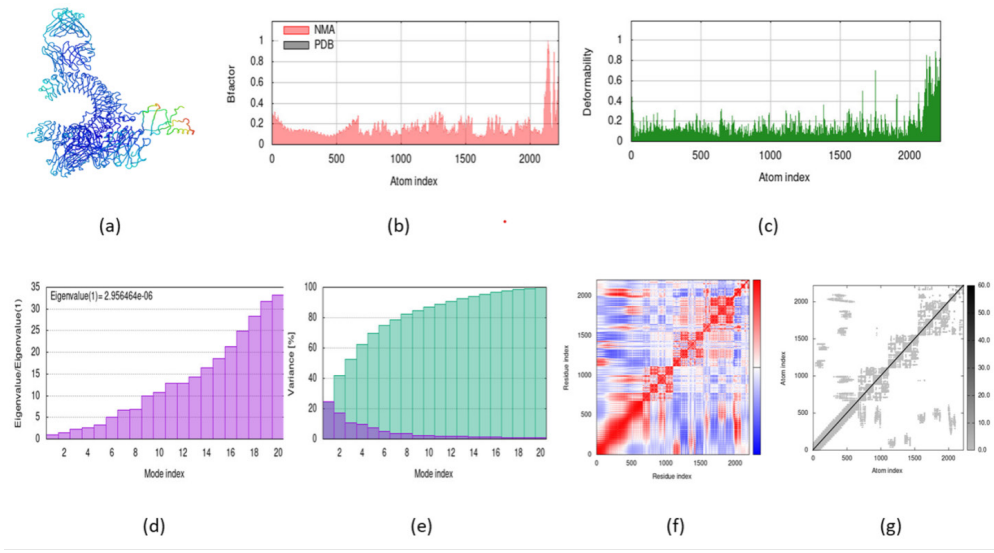

Figure 4. The results of the iMods simulation study of the proposed mRNA vaccine and TLR-3 docked complex. (a) MNA mobility, (b) deformability, (c) B factor, (d) Eigen values, (e) variance (green color indicated cumulative variances and purple color indicates the individual variance), (f) co-variance map (uncorrelated as white, correlated as red, and anti-correlated as blue motions) and (g) elastic network (darker grey regions indicate stiffer regions).

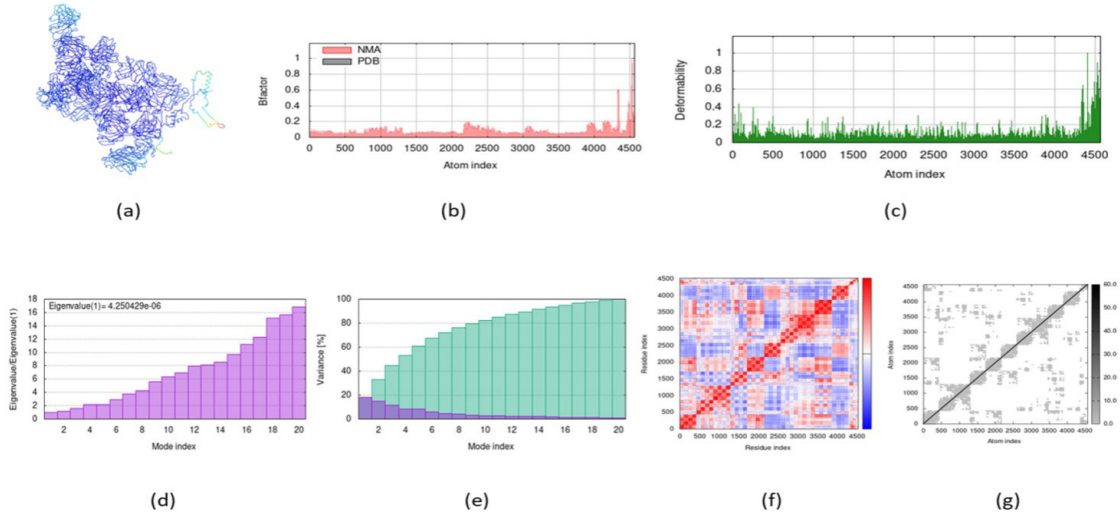

Figure 5. The results of the iMods simulation study of the proposed mRNA vaccine and TLR-4 docked complex. (a) MNA mobility, (b) deformability, (c) B factor, (d) Eigen values, (e) variance (green color indicated cumulative variances and purple color indicates the individual variance), (f) co-variance map (uncorrelated as white, correlated as red, and anti-correlated as blue motions) and (g) elastic network (darker grey regions indicate stiffer regions)

gies being present, this study proposed a mRNA-based vaccine design to develop protective immunity against the pathogen. This effort was in line with the previous studies proposing protective immunity against diseases (Al Tbeishat *et al*., 2022) like mucormycosis (Maruggi *et al*., 2017) and HPIV-1 (Naveed *et al*., 2022). Recently, COVID-19 RNA-based vaccines like Pfizer-BioNtech's 'Comirnaty' have worked wonders by developing prior immunity in the human body against the SARS-Cov-2 attack (Rotshild *et al*., 2021). It has been observed that vaccines have some epigenetic impact on immune system genes, which train the immune system (Kumar *et al*., 2015). Likewise, the focus of this study was to develop a long-lasting memory in the form of activated B cells and T cells. The HTL induces IL-10, IL-4, and IFN-γ, antigen-presenting cells express epitopes of HTL, and the lymphocyte can secrete chemokines, all play crucial roles against the virus (Al Tbeishat *et al*., 2022). We observed the production of all these immune system components in response to the antigen. Except for the memory cells, all the immune cells died and were eliminated with the destroyed antigen. B cells with membrane-bound immunoglobulin receptors identified the antigen epitopes and internalized them to become presenting cells for memory-making units of the immune system. Furthermore, we noticed a hike in plasma-secreted antibodies (up to 40 000 counts) that are utilized to neutralize the antigen (vaccine candidate injection) and produce memory cells. Our results were consistent with previous mRNA-based vaccine findings (Naveed *et al*., 2022; Maruggi *et al*., 2017), predicting an efficacious vaccine construct with the ability to elicit long-lasting protective immunity.

The tools utilized in this study have revolutionized biotechnological research. The reverse-vaccinology ap-

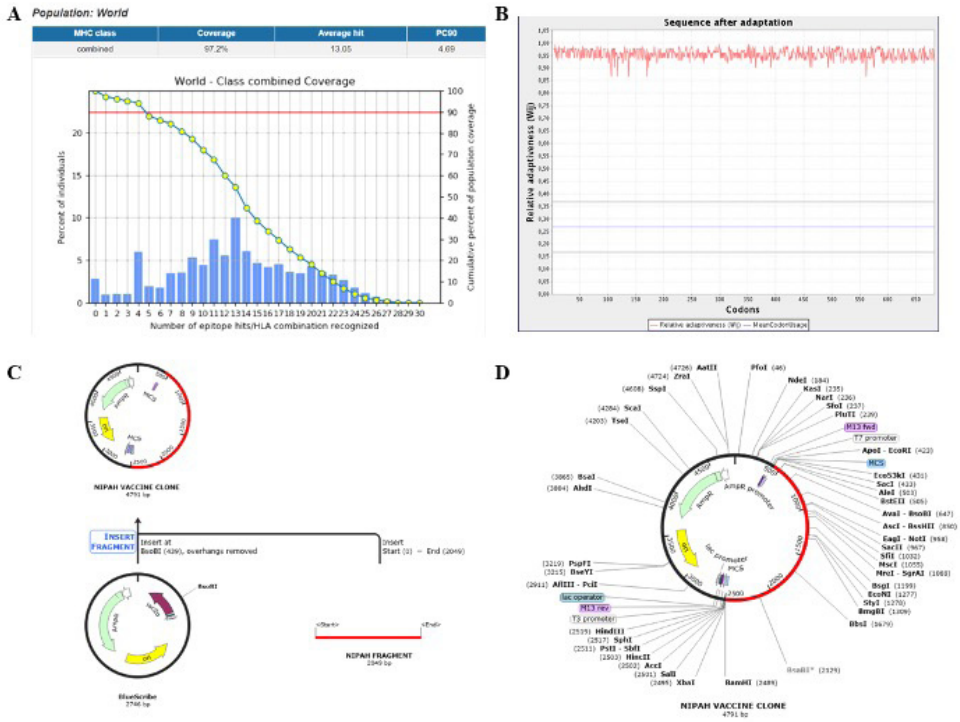

Figure 6. (A) Population coverage of the T-cell-specific epitopes; (B) Codon optimization chart of the proposed mRNA vaccine construct; (C) The history map of cloning, the black vector shows pBluescribe plasmid, 2040 bps long, the red line shows vaccine construct and the final construct after insertion in which red color shows gene of interest (4791 bps long); (D) The cloned Bluescribe vector with the gene of interest shown in red color

proach has saved time, preliminary clinical trials, and labor costs (Kumar *et al*., 2015). We followed this approach because of its proclaimed merits in prediction ((Naveed *et al*., 2022a; Naveed *et al*., 2022b) as well as clinical studies (Hall *et al*., 2021; Pormohammad *et al*., 2021). The *in-silico* prediction of antigenicity, allergenicity, and toxicity significantly helped us in characterizing the potential epitopes. These tools have the potential to save lives at pre-clinical trials (Xinhui *et al*., 2021) as researchers may have already predicted the immunogenic, allergenic, or toxic outcome of a proposed vaccine before it is administered to the public (Naveed *et al*., 2023a; Naveed *et al*., 2023b). Lastly, the wide population coverage of the proposed candidate validates that it can be efficacious worldwide irrespective of race, ethnicity, or area.

Declarations

Ethics approval and consent to participate: Not applicable.

Competing interests: The authors declare no conflict of interest.

Funding: No external funding was received.

Authors' contributions: Conceptualization, M.N. and S.M.; methodology, M.H.A; software, U.A.; validation, F.N., and T.A.; formal analysis, M.N; investigation, U.A and S.M.; resources, M.N.; data curation, M.S and M.E.A.; writing – original draft preparation, M.A and C.Z; writing – review and editing, T.A.; visualization, M.A. A.F.A, and A.A.S; supervision, T.A.; project administration, M.N.; funding acquisition, T.A.

Availability of data and material: All the data used in this research work has been included in this manuscript.

REFERENCES

Aditi, Shariff M (2019) Nipah virus infection: A review. *Epidemiol. Infect.* **147**. https://doi.org/10.1017/S0950268819000086

Al Tbeishat H (2022) Novel *in silico* mRNA vaccine design exploiting proteins of *M. tuberculosis* that modulates host immune responses by inducing epigenetic modifications. *Sci. Rep.* **12**. https://doi.org/10.1038/s41598-022-08506-4

Deb S, Vyas DB, Pendharkar AV, Rezaii PG, Schoen MK, Desai K, Gephart MH, Desai A (2019) Socioeconomic predictors of pituitary surgery. *Cureus* **11**: e3957. https://doi.org/10.7759%2Fcureus.3957

Fischer K, Diederich S, Smith G, Reiche S, Pinho dos Reis V, Stroh E, Groschup MH, Weingartl HM, Balkema-Buschmann A (2018) Indirect ELISA based on Hendra and Nipah virus proteins for the detection of henipavirus specific antibodies in pigs. *PLoS One* **13**: e0194385. https://doi.org/10.1371/journal.pone.0194385

Hall VG, Ferreira VH, Ku T, Ierullo M, Majchrzak-Kita B, Chaparro C, Selzner N, Schiff J, McDonald M, Tomlinson G, Kulasingam V, Kumar D, Humar A (2021) Randomized trial of a third dose of mRNA-1273 vaccine in transplant recipients. *N. Engl. J. Med.* **385**: 1244–1246. https://doi.org/10.1056/NEJMc2111462

Kulkarni DD, Tosh C, Venkatesh G, Senthil Kumar D (2013) Nipah virus infection: current scenario. *Virusdisease* **24**: 398–408. https://doi.org/10.1007/s13337-013-0171-y

Kumar G, Menanteau-Ledouble S, Saleh M, El-Matbouli M (2015) *Yersinia ruckeri*, The causative agent of enteric redmouth disease in fish. *Vet. Res.* **46**. https://doi.org/10.1186/s13567-015-0238-4

Leman JK, Weitzner BD, Lewis SM, Adolf-Bryfogle J, Alam N, Alford RF, Aprahamian M, Baker D, Barlow KA, Barth P, Basanta B, Bender BJ, Blacklock K, Bonet J, Boyken SE, Bradley P, Bystroff C, Conway P, Cooper S, Correia BE (2020) Macromolecular modeling and design in Rosetta: recent methods and frameworks. *Nat. Methods* **17**: 665–680. https://doi.org/10.1038/s41592-020-0848-2

Maruggi G, Chiarot E, Giovani C, Buccato S, Bonacci S, Frigimelica E, Margarit I, Geall A, Bensi G, Maione D (2017) Immunogenicity and protective efficacy induced by self-amplifying mRNA vaccines encoding bacterial antigens. *Vaccines* **35**: 361–368. https://doi.org/10.1016/j.vaccine.2016.11.040

Mourya DT, Yadav P, Sudeep AB, Gokhale, MD, Gupta, N, Gangakhedkar RR, Bhargava B (2018) Spatial association between a nipah virus outbreak in India and nipah virus infection in pteropus bats. *Clin. Infect. Dis.* **69**: 378–379. https://doi.org/10.1093/cid/ciy1093

Naveed M, Mughal MS, Jabeen K, Aziz T, Naz S, Nazir N, Shahzad M, Alharbi M, Alshammari A, Sadhu SS (2022) Evaluation of the whole proteome to design a novel mRNA-based vaccine against multidrug-resistant *Serratia marcescens*. *Front. Microbiol.* **13**: 960285. https://doi.org/10.3389/fmicb.2022.960285

Naveed M, Tehreem S, Arshad S, Bukhari SA, Shabbir MA, Essa R, Ali N, Zaib S, Khan A, Al-Harrasi A, Khan I (2021) Design of a novel multiple epitope-based vaccine: An immunoinformatics approach to combat SARS-CoV-2 strains *J. Infect. Public Health* **14**: 938–946. https://doi.org/10.1016/j.jiph.2021.04.010

Naveed M, Ain N, Aziz T, Ali I, Aqib Shabbir M, Javed K, Alharbi M, Alshammari A, Alasmari AF (2023) Revolutionizing treatment for toxic shock syndrome with engineered super chromones to combat antibiotic-resistant *Staphylococcus aureus*. *Eur. Rev. Med. Pharmacol. Sci.* **27**: 5301–5309. https://doi.org/10.26355/eurrev_202306_32649

Naveed M, Ain N, Aziz T, Javed K, Ishfaq H, Khalil S, Alharbi M, Alshammari A, Alasmari AF (2023) Pharmacophore screening approach of homeopathic phenols for a renovated design of fragment-optimized Bauhiniastatin-1 as a drug against acromegaly. *Eur. Rev. Med. Pharmacol. Sci.* **27**: 5530–5541. https://doi.org/10.26355/eurrev_202306_32790.

Naveed M, Ali U, Karobari MI, Ahmed N, Mohamed RN, Abullais SS, Kader MA, Marya A, Messina P, Scardina GA (2022) A vaccine construction against COVID-19-associated mucormycosis contrived with immunoinformatics-based scavenging of potential mucoralean epitopes. *Vaccines* **10**: 664. https://doi.org/10.3390/vaccines10050664

Naveed M, Jabeen K, Naz R, Mughal MS, Rabaan AA, Bakhrebah MA, Alhoshani FM, Aljeldah M, Shammari BRA, Alissa M, Sabour AA, Alaeq RA, Alshiekheid MA, Garout M, Almogbel MS, Halwani MA, Turkistani SA, Ahmed N (2022) Regulation of host immune response against enterobacter cloacae proteins *via* computational mRNA vaccine design through transcriptional modification. *Microorganisms* **10**: 1621. https://doi.org/10.3390/microorganisms10081621

Naveed M, Sheraz M, Amin A, Waseem M, Aziz T, Khan AA, Ghani M, Shahzad M, Alruways MW, Dablool AS, Elazzazy AM, Almalki AA, Alamri AS, Alhomrani M (2022) Designing a novel peptide-based multi-epitope vaccine to evoke a robust immune response against pathogenic multidrug-resistant *Providencia heimbachae*. *Vaccines* **10**: 1300. https://doi.org/10.3390/vaccines10081300

Naveed M, Shabbir MA, Ain N-u, Javed K, Mahmood S, Aziz T, Khan AA, Nabi G, Shahzad M, Alharbi ME, Alharbi M, Alsahammari A (2022) Chain-engineering-based *de novo* drug design against MPX-Vgp169 virulent protein of monkeypox virus: a molecular modification approach. *Bioengineering* **10**: 11. https://doi.org/10.3390/bioengineering10010011

Naveed M, Ain Nu, Aziz T, Javed K, Shabbir MA, Alharbi M, Alsahammari A, Alasmari AF (2023) Artificial intelligence assisted pharmacophore design for philadelphia chromosome-positive leukemia with gamma-tocotrienol: a toxicity comparison approach with asciminib. *Biomedicines* **11**: 1041. https://doi.org/10.3390/biomedicines11041041

Naveed M, Waseem M, Aziz T, Hassan Ju, Makhdoom SI, Ali U, Alharbi M, Alsahammari A (2023) Identification of bacterial strains and development of anmrna-based vaccine to combat antibiotic resistance in *Staphylococcus aureus via in vitro* and *in silico* approaches. *Biomedicines* **11**: 1039. https://doi.org/10.3390/biomedicines11041039

Pillai VS, Krishna G, Valiya Veettil, M (2020) Nipah virus: past outbreaks and future containment. *Viruses* **12**: 465. https://doi.org/10.3390/v12040465

Pormohammad A, Zarei M, Ghorbani S, Mohammadi M, Razizadeh MH, Turner DL, Turner RJ (2021) Efficacy and safety of COVID-19 vaccines: a systematic review and meta-analysis of randomized clinical trials. *Vaccines* **9**: 467. https://doi.org/10.3390/vaccines9050467

Reddy K (2018) Nipah Virus (NiV) Infection: an emerging zoonosis of public health concern. *J. Gandaki Med. Coll. Nepal.* **11**. https://doi.org/10.3126/jgmcn.v11i02.22897

Reynisson B, Alvarez B, Paul S, Peters B, Nielsen M (2020) NetMHCpan-4.1 and NetMHCIIpan-4.0: improved predictions of MHC antigen presentation by concurrent motif deconvolution and integration of MS MHC eluted ligand data. *Nucl. Acids. Res.* **48**: W449–W454. https://doi.org/10.1093/nar/gkaa379

Rockx B, Bossart KN, Feldmann F, Geisbert JB, Hickey AC, Brining D, Callison J, Safronetz D, Marzi A, Kercher L, Long D, Broder CC, Feldmann H, Geisbert TW (2010) A novel model of lethal Hendra virus infection in African Green monkeys and the effectiveness of Ribavirin treatment. *J. Virol.* **84**: 9831–9839. https://doi.org/10.1128/JVI.01163-10

Sharma V, Kaushik S, Kumar R, Yadav JP, Kaushik S (2018) Emerging trends of Nipah virus: A review. *Rev. Med. Virol.* **29**: e2010. https://doi.org/10.1002/rmv.2010

Singh RK, Dhama K, Chakraborty S, Tiwari R, Natesan S, Khandia R, Munjal A, Vora KS, Latheef SK, Karthik K, Singh Malik, Singh R, Chaicumpa W, Mourya DT (2019) Nipah virus: epidemiology, pathology, immunobiology and advances in diagnosis, vaccine designing and control strategies – a comprehensive review. *Vet. Q.* **39**: 26–55. https://doi.org/10.1080/01652176.2019.1580827

Weingartl HM, Berhane Y, Czub M (2009) Animal models of henipavirus infection: A review. *Vet. J.* **181**: 211–220. https://doi.org/10.1016/j.tvjl.2008.10.016

Xinhui Cai, Jiao Jiao Li, Tao Liu, Oliver Brian, Jinyan Li (2021) Infectious disease mRNA vaccines and a review on epitope prediction for vaccine design. *Brief. Funct. Genom.* **20**: 289–303. https://doi.org/10.1093/bfgp/elab027

Zhang C, Maruggi G, Shan H, Li J (2019) Advances in mRNA vaccines for infectious diseases. *Front. Immunol.* **10**. https://doi.org/10.3389/fimmu.2019.00594